Spectral Energy Distribution(SED) Fitting of the Sparkler Galaxy

Most. Atia Sanjida

University of Dhaka

MS Student, Department of Physics

Session: 2023-2024

Supervised by,

Prof. Lamiya Mowla

Assistant Professor of Astronomy

Physics and Astronomy, Wellesley College

Whitin Observatory, OBS 112

www.mowlaastrogroup.com

Abstract

We present a near-infrared spectral energy distribution (SED) analysis of the Sparkler galaxy at z = 1.38 using PSF-matched JWST/NIRCam photometry and the non-parametric Dense Basis framework. Imaging was supplied as BCG-removed mosaics; source-centered 5″×5″ cutouts were generated via FITS-WCS. Two RGB composites (R=F200W/G=F150W/B=F090W and R=F444W/G=F356W/B=F277W) supported morphology/neighbor inspection; Photometry was performed in F090W–F444W after PSF matching all bands to the F444W resolution (FWHM ≈ 5.055 px) and applying a single elliptical aperture (defined on F444W) with robust local-sky subtraction. Filter transmission curves were assembled from the STScI NIRCam throughput archive, converted to Å, and supplied to Dense Basis. We adopted Sparkler-specified priors on stellar mass, SFH (three-parameter non-parametric family with sSFR-flat prior), metallicity, dust attenuation, and redshift; a model atlas was generated, and posteriors were evaluated to derive 16th–50th–84th percentile constraints. This workflow yields credible estimates of the galaxy's stellar mass, mass-weighted age/SFH, metallicity, and attenuation while transparently propagating photometric uncertainties and SFH flexibility. We discuss parameter degeneracies (age–dust–metallicity), prior sensitivities, and practical considerations for non-parametric SED fitting in small, isolated cutouts.

1. Introduction

Constraining the buildup of stellar mass and the regulation of star formation in the early universe requires rest-frame optical–near-IR measurements that are sensitive to stellar mass, mass-weighted age, metallicity, and dust. JWST/NIRCam now delivers this leverage at high redshift, and when combined with strong gravitational lensing, the effective depth and spatial resolution improve further, bringing intrinsically faint systems within reach. In this context, the **Sparkler** is especially valuable: it is a compact galaxy at $z_{spec} \approx 1.378$ that is **strongly lensed** by the foreground cluster **SMACS J0723.3–7327** ($z = 0.39$), enabling detailed photometric study that would otherwise be prohibitive.

Initial JWST studies of the Sparkler highlighted numerous compact, red companions ("sparkles") plausibly consistent with evolved globular cluster candidates, identified across multiple lensed images and exhibiting colors and sizes consistent with old, quenched stellar systems. Those works combined HST and JWST imaging with SED modeling to infer early formation epochs for the compact sources. In the present work, however, we focus exclusively on the host galaxy's integrated SED, not on the surrounding compact companions, leveraging lensing-aided JWST photometry to infer the galaxy's stellar population properties.

Methodologically, we employ PSF-matched aperture photometry on BCG-subtracted mosaics and a non-parametric SED framework (Dense Basis) to mitigate biases from restrictive SFH forms while transparently propagating photometric uncertainties through full posteriors. This design is motivated by the potential complexity of high-z star-formation histories and by the wavelength coverage of our NIRCam bands (F090W–F444W), which together provide leverage against age–dust–metallicity degeneracies. Our objectives are to (i) construct a reproducible,

PSF-matched photometric catalog for the Sparkler, (ii) fit non-parametric SFHs with clearly stated priors, and (iii) report posterior constraints on stellar mass, mass-weighted age/SFH, metallicity, and dust attenuation, placing the results in the context of prior work on the system.

2. Data and Photometry

2.1 Observational data

The photometric data for the Sparkler Galaxy used in this work were provided by my mentor, **Prof. Lamiya Mowla**, as BCG-removed mosaics, in which the diffuse light from the brightest cluster galaxy and associated intracluster background had been subtracted. The delivered products consisted of calibrated JWST/NIRCam FITS frames. No pre-extracted target cutout was supplied; instead, source-centered cutouts were generated directly from the BCG-removed FITS using the FITS WCS solutions.

For visualization, I opted for a DS9-like display. So, I used astropy.visualization, ZScaleInterval, ImageNormalize, and LinearStretch, choosing zscale-derived limits rather than statistics-based (e.g., median) for vmin/vmax. I set Z_CONTRAST = 0.075 and stretch = LinearStretch(), which after experimentation, provided superior contrast and detail for inspecting faint residual structures and neighboring sources in the BCG-subtracted fields. These settings affected plots only and were not used in any flux measurement, background estimation, or SED-fitting steps.

2.2 Filters

Photometric measurements for SED fitting were performed exclusively in the JWST/NIRCam wide bands F090W, F115W, F150W, F200W, F277W, F356W, and F444W. Central wavelengths are listed for reference:

Filter	Central λ (μm)
F090W	0.90
F115W	1.15
F150W	1.50
F200W	2.00
F277W	2.77
F356W	3.56
F444W	4.44

These bands provide continuous near-IR coverage for robust SED constraints on the galaxy's stellar continuum, dust attenuation, and age-sensitive spectral breaks. F090W–F200W sample the blue/near-IR continuum and bracket age-sensitive breaks for typical high-z systems; they also can be affected by Balmer/Hα/[O III]+Hβ if those lines fall in-band at the source redshift. F277W–F444W capture the redder continuum that anchors the stellar mass estimate and are less sensitive to short-timescale SFR variations, while still susceptible to strong lines if present. This division provides leverage against common SED degeneracies (age–dust–metallicity) in the near-IR.

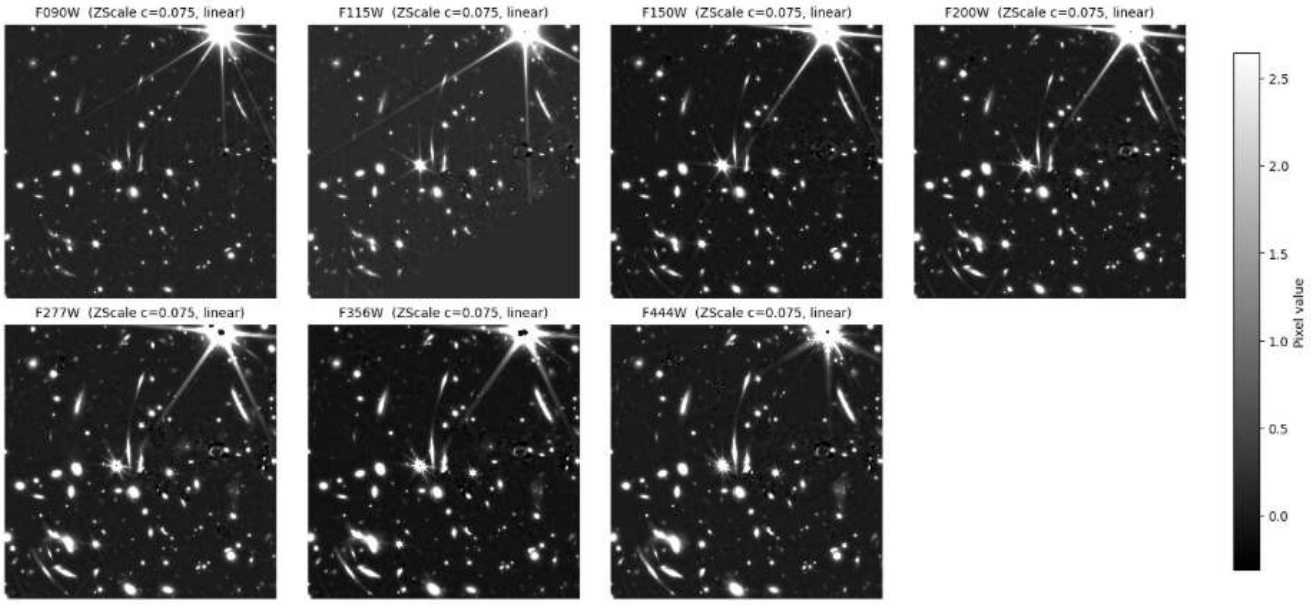

Fig.1 : BCG_removed fits data across 7 filters (F090 - F444W) in gray scale

2.3 5″ × 5″ Cutout construction of the Sparkler galaxy for all filters

For each band, a square 5″ × 5″ cutout enclosing the full galaxy light and an adequate background region was produced using the FITS WCS. The astrometric reference was the F444W filter: the target centroid was identified in DS9, and its sky coordinates were recorded. For reproducibility, the detector coordinates used for the cutout center were (x, y) = (627, 616.536) pixels. Cutouts in all remaining filters were extracted with the same sky center using astropy.nddata.Cutout2D, ensuring identical footprint and aperture placement across bands. All cutouts were then co-registered to a common astrometric frame via the WCS transformations (with F444W as the reference) to guarantee pixel-level alignment. Visual quality checks confirmed (i) consistent centroiding across filters, (ii) absence of strong BCG-subtraction residuals within the photometric aperture, and (iii) no truncation at image boundaries.

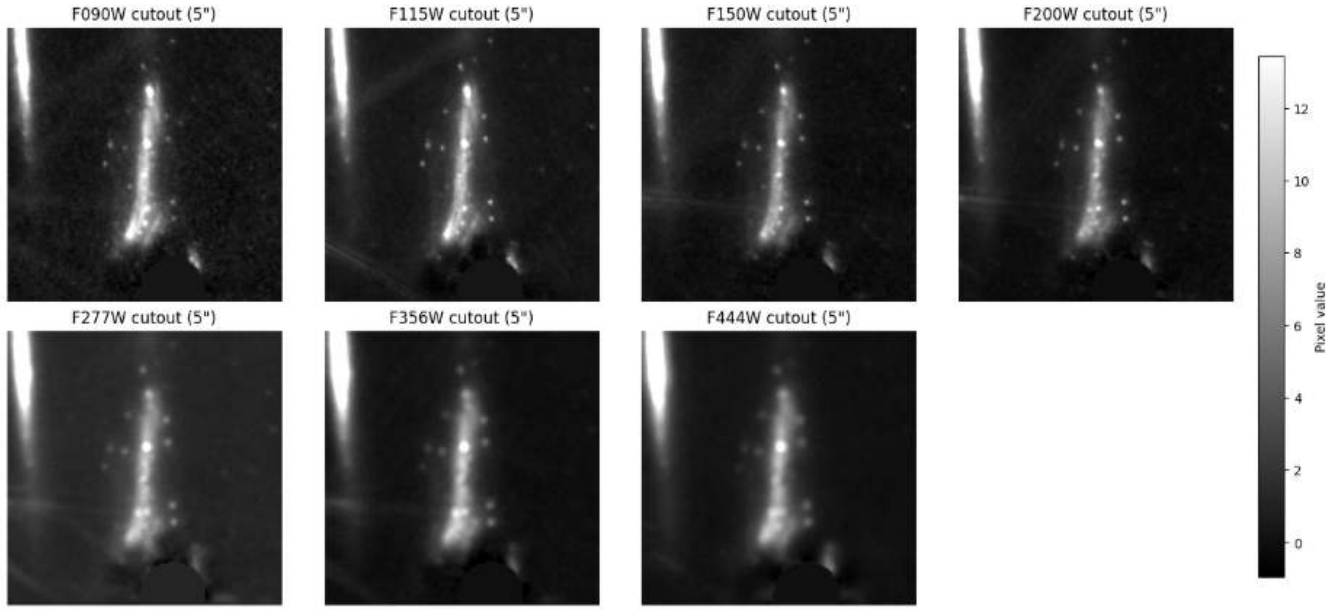

Fig.2 : The Sparkler Galaxy in 5″ × 5″ cutout across all 7 filters (F090 - F444W) in gray scale

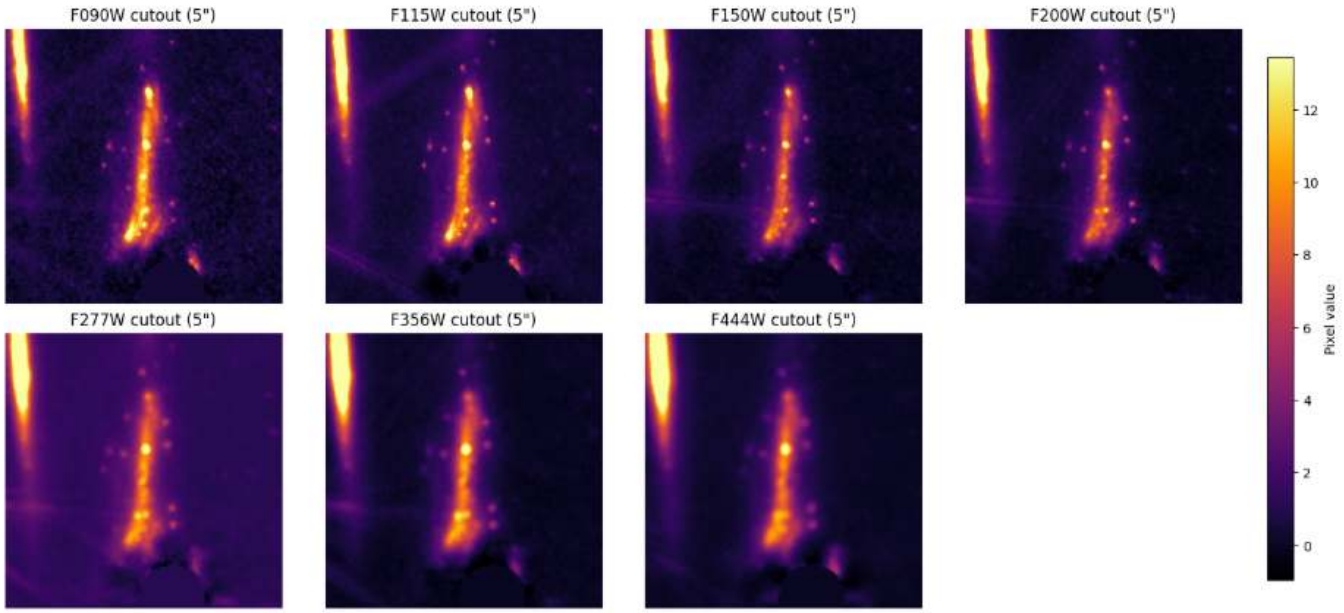

Fig.3 : The Sparkler Galaxy in 5″ × 5″ cutout across all 7 filters (F090 - F444W) in inferno scale

2.4 RGB composites for visual quality assurance

Two false-color images were created to assess morphology, blending, and residual backgrounds prior to photometry:

RGB-1: R = F200W, G = F150W, B = F090W

RGB-2: R = F444W, G = F356W, B = F277W

These complementary combinations emphasize blue–near-IR structure (RGB-1) and redder continuum morphology (RGB-2), aiding the identification of artifacts or neighbors that could bias aperture placement.

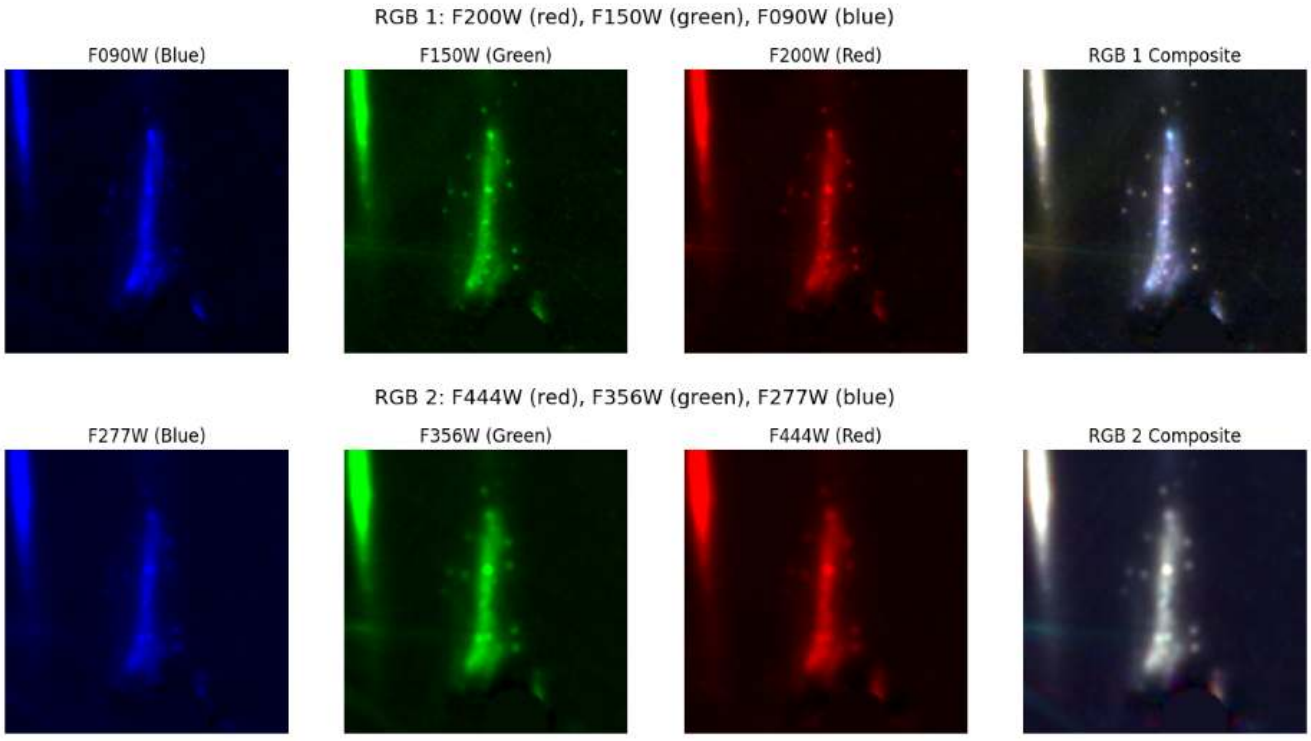

Fig.4: Preparing RGB images by combining 3 filter data

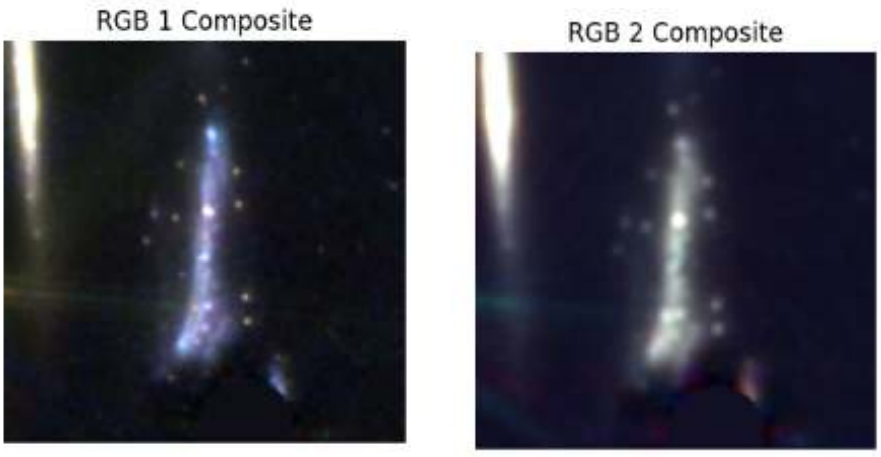

Fig.5: Two RGB images (for side-by-side comparison)

2.5 Photometric catalog

Photometry was carried out on the aligned, BCG-removed cutouts in F090W–F444W and compiled into a band-merged catalog reporting flux density (nJy) and 1σ uncertainties per filter. Procedural details (aperture definition, background estimation, PSF homogenization and aperture corrections, unit conventions, and uncertainty propagation) are provided in the Methodology.

3. Methodology

3.1 Photometric Process

The photometric measurements for the Sparkler Galaxy were performed in a stepwise manner, ensuring accurate flux extraction while accounting for background variations and instrumental effects. The following steps outline the procedure.

3.1.1 Background Estimation and Image Preparation

First, the background for each of the seven filters (F090W to F444W) was estimated. The background was calculated using the median sky values across the cutout regions of each image. For each filter, the following images were generated:

- The cutout image of Sparkler
- The background model (estimated background), and
- The background-subtracted image.

These images were visually inspected to ensure accurate background subtraction, with clear separation between source light and sky noise. The images were then used for subsequent photometric analysis.

3.1.2 Defining Elliptical Aperture over Sparkler Galaxy in F444W filter cutout by Adaptive Ellipse Growth

The next step involved selecting a central region in the F444W filter cutout. The F444W filter is chosen as it represents the far-infrared wavelength regime. A central segment of the galaxy was selected, and an adaptive elliptical growth method was applied to define the photometric aperture. This process allowed for a precise delineation of the galaxy's light distribution,

especially important given the complex morphology of the target. The final adaptive ellipse was overlaid on the image, and a coverage report was generated to ensure that the aperture accurately encompassed the galaxy's light while avoiding contamination from neighboring sources.

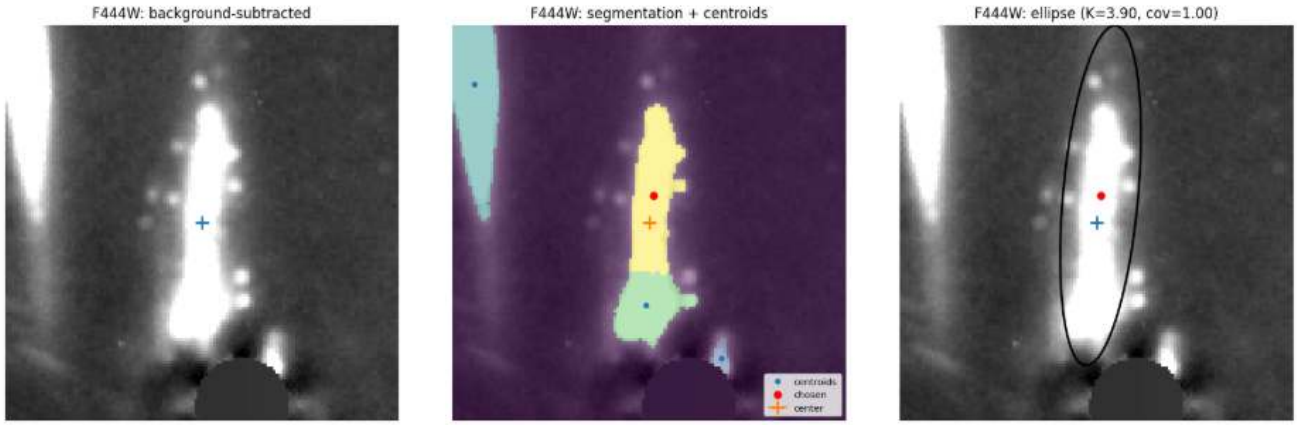

Fig.6: Defining Elliptical Aperture over Sparkler Galaxy in F444W filter cutout

3.1.3 PSF Matching and Convolution

To ensure consistent photometry across all filters, PSF matching was performed with respect to the F444W filter, as it was chosen as the reference band due to its placement in the far-infrared. The Point Spread Function (PSF) was matched for all filters based on the FWHM (Full Width at Half Maximum) derived from the full mosaics. The FWHM for the F444W filter was estimated to be 5.055 pixels.

A PSF convolution was then applied to the rest of the filter's cutouts. The PSF matching was performed by convolving the other filter images to match the resolution of the F444W cutout. This ensured that all photometric measurements were conducted under consistent spatial resolution, reducing biases due to instrumental differences.

3.1.4 Elliptical Aperture Photometry

Following PSF matching, elliptical-aperture photometry was performed on the PSF-matched cutouts. The photometry was carried out with robust sky background estimation, using the previously computed background models for each filter. The fluxes were measured within the elliptical apertures, ensuring that the galaxy's light profile was accurately captured while accounting for the variation in PSF and background across the different filters.

A catalog, catalog_psf, was generated and saved as a CSV file, containing the flux values, flux uncertainties, and other relevant parameters for each filter. The final catalog served as the input for the SED fitting process.

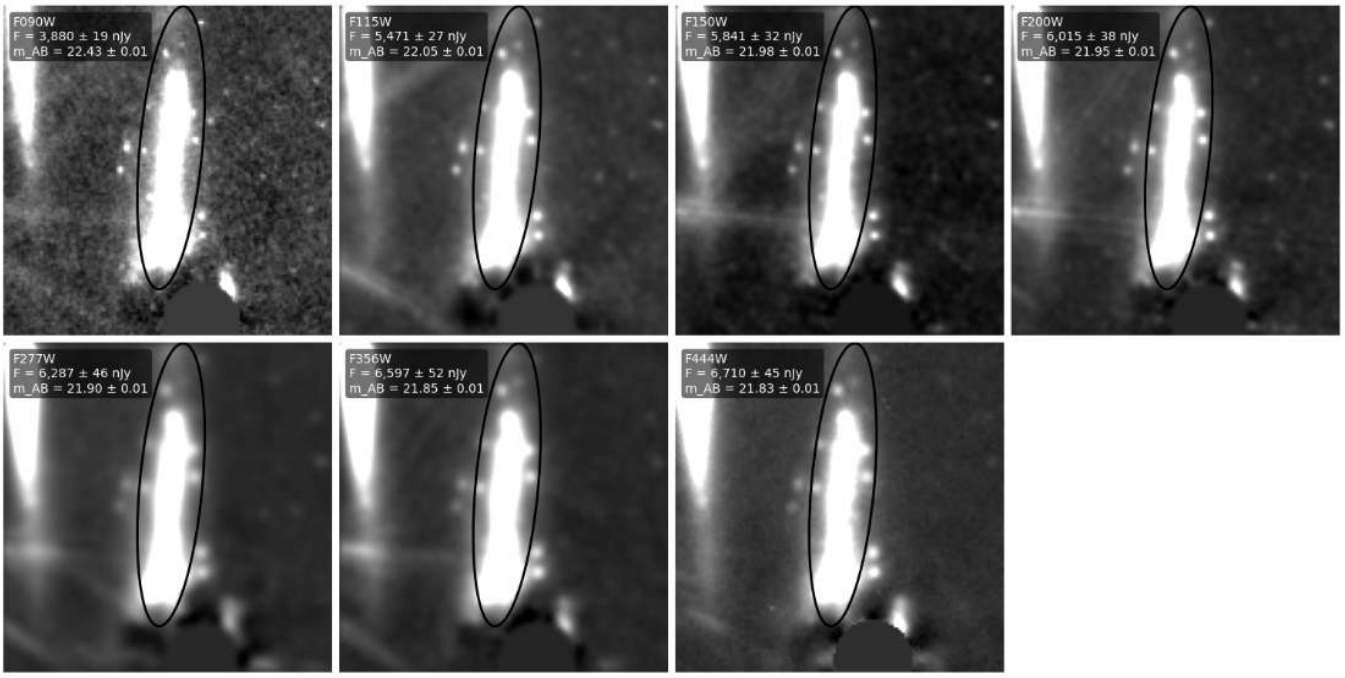

Fig.7: PSF-matched cutouts with ellipse + flux ± error overlays

	filter	flux_nJy	flux_err_nJy	Npix	bkg_rms_median_nJy	f_corr	n_random_used
0	F090W	3879.613228	19.484452	2027	0.426224	1.0	0
1	F115W	5471.057658	26.750345	2027	0.593518	1.0	0
2	F150W	5841.313983	31.607102	2027	0.703242	1.0	0
3	F200W	6014.602485	37.587082	2027	0.775152	1.0	0
4	F277W	6287.087959	45.733419	2027	0.948070	1.0	0
5	F356W	6597.024558	52.446429	2027	1.055191	1.0	0
6	F444W	6710.004023	44.973449	2027	0.927386	1.0	0

Fig.8: Flux and flux error of the Sparkler galaxy in nJy catalog_psf data

3.1.5 Conversion to Magnitudes

To facilitate the SED fitting, the fluxes and associated uncertainties were converted from nJy (nanoJanskys) to AB magnitudes. The conversion was performed using the standard relation:

$$m_{AB} = -2.5log(f_v) + 31.4$$

where f_v is the flux in units of nJy. The resulting magnitudes and magnitude uncertainties were stored in a separate CSV file, providing the required format for input into the SED fitting analysis.

	filter	flux_nJy	flux_err_nJy	Npix	bkg_rms_median_nJy	f_corr	n_random_used	mag_AB	mag_err
0	F090W	3879.613228	19.484452	2027	0.426224	1.0	0	22.428029	0.005453
1	F115W	5471.057658	26.750345	2027	0.593518	1.0	0	22.054822	0.005308
2	F150W	5841.313983	31.607102	2027	0.703242	1.0	0	21.983724	0.005875
3	F200W	6014.602485	37.587082	2027	0.775152	1.0	0	21.951983	0.006785
4	F277W	6287.087959	45.733419	2027	0.948070	1.0	0	21.903876	0.007898
5	F356W	6597.024558	52.446429	2027	1.055191	1.0	0	21.851630	0.008631
6	F444W	6710.004023	44.973449	2027	0.927386	1.0	0	21.833193	0.007277

Fig.9: Flux and flux error of the Sparkler galaxy in magnitudes, converting from nJy

3.1.6 Aperture strategy (no segmentation map, detect_sources, deblending)

Rather than constructing a segmentation map and computing isophotal fluxes, I measured fluxes directly within a single elliptical aperture. This choice is motivated by the data geometry: each 5″×5″ cutout contains a single, prominent, centrally located galaxy (the Sparkler), making a fixed ellipse more appropriate and stable than segmentation/deblending. The aperture was defined on the F444W reference image via adaptive ellipse growth to capture the galaxy's light while excluding residual artifacts; the derived ellipse (center, PA, axis ratio, semi-major axis) was held fixed across filters and applied after PSF matching. Fluxes and uncertainties were computed within this aperture using the robust sky procedure, ensuring consistent colors and minimizing model-dependent deblending systematics.

3.1.7 Photometry Ready for SED Fitting

With the photometry completed, the data were prepared for SED fitting. To visually inspect the quality of the PSF-matched photometry, I plotted the PSF-matched cutouts with the elliptical apertures overlaid, along with flux ± error overlays for all seven filters (F090W to F444W). These visualizations ensure that the photometric apertures correctly trace the galaxy's light and that the flux measurements accurately reflect the background-subtracted counts. These steps confirm that the data are ready for the next stage of SED fitting.

3.2 SED Fitting

3.2.1 Model choice: Dense Basis

We adopt Dense Basis as the non-parametric SED model because it (i) represents SFHs with flexible bases (or GP-regularized trajectories) that capture diverse formation pathways; (ii)

encodes explicit priors on stellar mass, metallicity, dust, redshift, and SFH smoothness/variance; (iii) uses a precomputed atlas to enable fast, reproducible likelihood evaluation and posterior summaries; and (iv) returns credible intervals (16th–50th–84th percentiles) that transparently propagate photometric uncertainties and model degeneracies. For the Sparkler dataset, seven NIRCam bands with PSF-matched photometry—this choice leverages the near-IR continuum leverage for stellar mass while permitting recent/bursty activity without imposing a single decay timescale.

Advantages over parametric fits (in this context):

- Captures bursty or multi-phase SFHs without bias from an assumed form.
- Mitigates age–dust–metallicity confounding by marginalizing over a richer SFH family.
- Prior-aware: smoothness and amplitude priors prevent unphysical solutions while avoiding over-constraint.
- Computational efficiency & reproducibility via the atlas and fixed filter set.

4. SED Fitting with Dense Basis

4.1 Filter Transmission Curves and Setup

To begin the SED fitting process, the filter transmission curves for each of the observed filters (F090W to F444W) were obtained from the NIRCam throughput archive provided by the Space Telescope Science Institute (STScI). For each of the filters used in the observations, I downloaded the corresponding transmission curves and created individual text files (e.g., JWST_F090W.txt, JWST_F150W.txt, ... JWST_F444W.txt) for each filter. These files were then

aggregated into a filter list file, my_jwst_filters.dat, which was used as input for the SED fitting process.

A visual representation of the filter transmission curves was produced by plotting the overlay of all the filters, which allowed for an assessment of the wavelength coverage of the SED fitting model. This overlay can be seen in the figure below

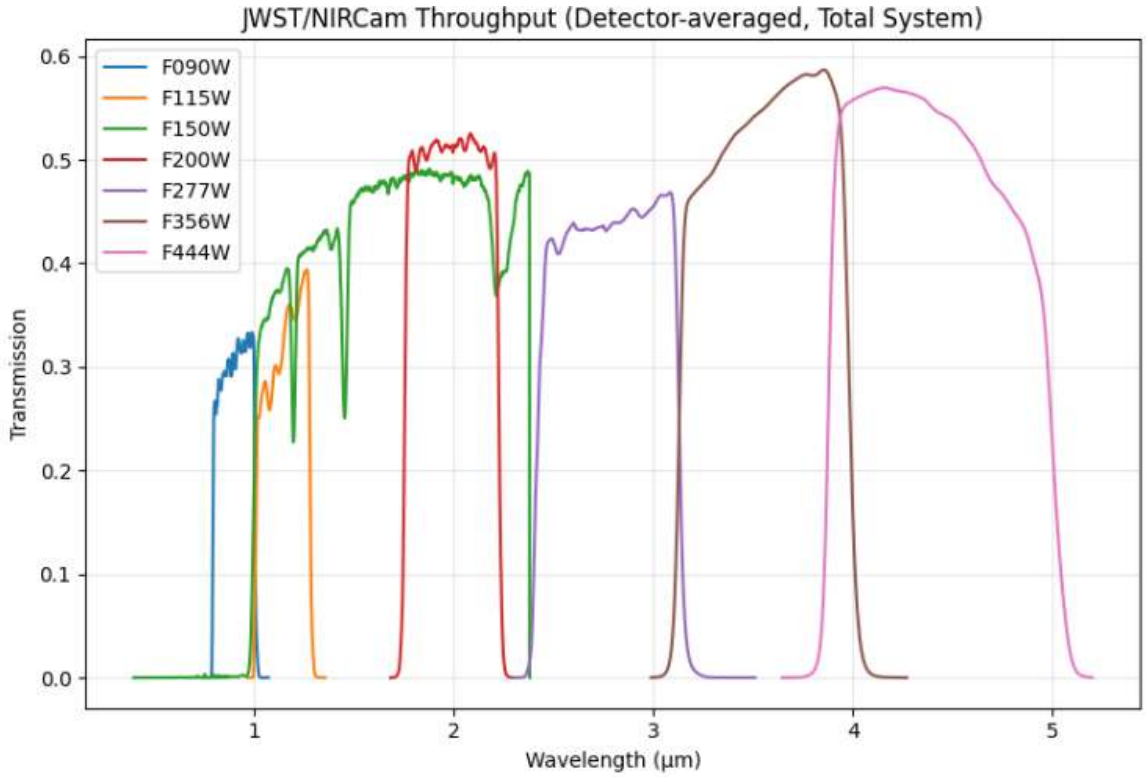

.

Fig.10: Overlay of JWST filter transmission curves.

4.2 Conversion of Wavelength Units

The wavelengths in the downloaded filter transmission curves were initially given in microns. To standardize the data for Dense Basis, all filter curve files were converted to Angstroms in-place. This conversion ensures compatibility with the SED fitting model, Dense Basis, which operates in the unit system of Angstroms for wavelength.

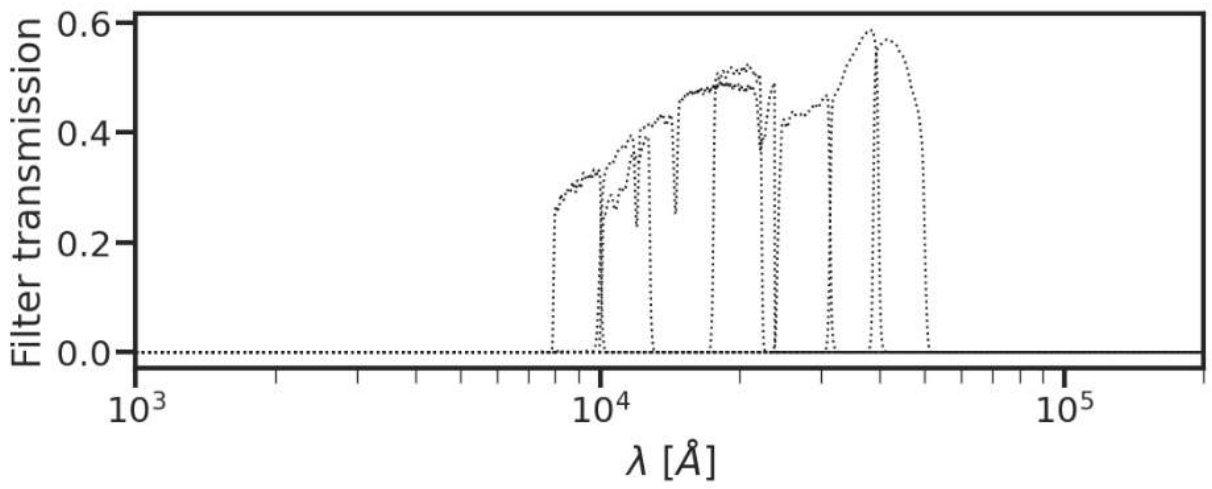

Fig.11: JWST filter transmission curves in Dense Basis from F090W-F444W

4.3 Photometric Data Preparation

Next, the photometric data in AB magnitudes obtained from the photometry process were loaded into the Dense Basis framework. The magnitudes were converted into flux units (μJy) before, ensuring proper scaling for the SED fitting. Additionally, the 1σ uncertainties from the photometric measurements were propagated to create the corresponding flux uncertainties (ferr_ujy). These flux values and their uncertainties formed the basis for the subsequent SED fitting procedure.

4.4 Priors Setup

To perform the SED fitting, I set the priors for the galaxy model using the parameter values provided by my mentor. The following priors were applied to the model:

- **Stellar Mass:** The prior for stellar mass was set to a logarithmic range between $log(M_*) = 5$ and $log(M_*) = 10$

- **Star Formation History (SFH):** The SFH priors were set with 3 parameters, with an exponential decline for the first parameter and a flat prior for the subsequent ones. The sSFR (specific star formation rate) prior was also set to a flat distribution, with a range of $-11 < sSFR < -6$
- **Metallicity:** A flat metallicity prior was applied, ranging from $Z = -1.0$ and $Z = 1.0$
- **Dust Attenuation:** An exponential dust prior was used, with A_V (the dust extinction in the V band) ranging from 0 to 4.
- **Redshift:** The redshift prior was fixed at $z = -1.38$, with a narrow range of $-1.375 < z < 1.385$

The prior settings allow for flexibility in the SED fitting while ensuring that the derived parameters remain physically plausible, based on our knowledge of galaxy evolution and previous studies.

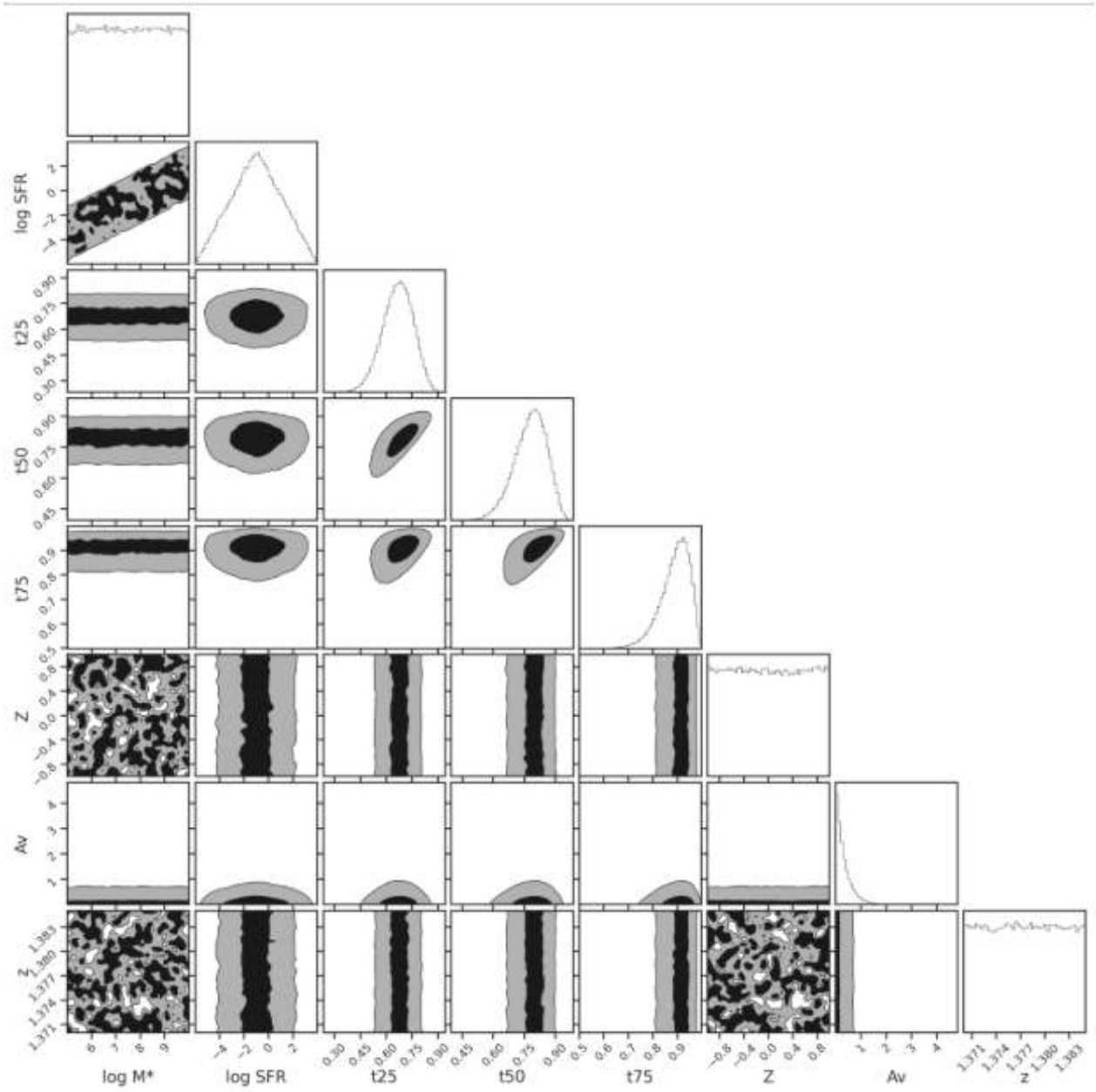

Fig.12: Corner plot showing prior distribution

4.5 Atlas Generation

Using the defined priors, the SED model atlas was generated. The atlas consists of a grid of model galaxies with varying parameters (such as stellar mass, age, metallicity, dust attenuation, and star formation rate), which serve as the reference for fitting the observed photometry. This

atlas provides the necessary model solutions for comparing against the observed data to evaluate the likelihood of each model.

4.6 SED Fitting and Posterior Analysis

Once the atlas was built, I loaded the model and performed the SED fitting using the Dense Basis framework. The photometric data were passed to the SedFit function, which uses the flux values and uncertainties along with the model atlas to compute the likelihood of each model. The fit was performed using the following command:

```
sedfit = db.SedFit(flux_ujy, ferr_ujy, atlas, fit_mask=fit_mask)
```

The posterior distributions for the galaxy's parameters (such as stellar mass, age, metallicity, and dust attenuation) were derived by evaluating the likelihood of each model solution using the evaluate_likelihood function. The posterior percentiles (16th, 50th, and 84th) were then calculated to summarize the results of the fit, providing a measure of uncertainty for the estimated parameters:

```
sedfit.evaluate_posterior_percentiles()
```

These posterior distributions, shown in Figure 2, represent the range of parameter values that are consistent with the observed data and the applied priors.

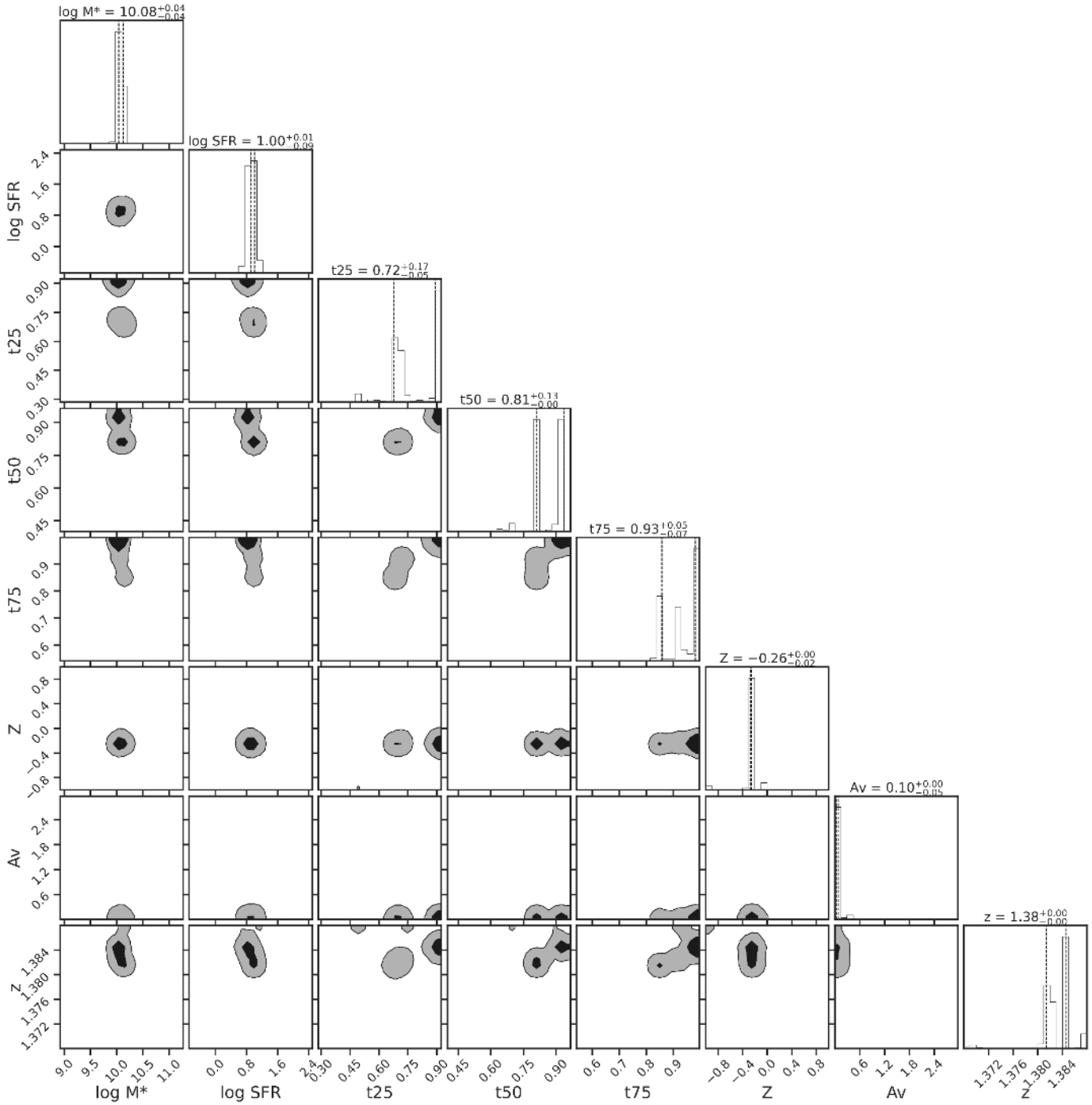

Fig.12: Corner plot showing posterior distribution

5. Results and Analysis

5.1 Results

The generated posterior distributions allowed for an in-depth analysis of the galaxy's physical properties, including its stellar mass, age, metallicity, and dust attenuation. Key findings from the posterior analysis were visualized and interpreted to understand the galaxy's evolutionary state.

The findings from my SED fitting analysis-

log10(M*/Msun): 10.017500000002011

log10(SFR): 1.1395000000023843

A_V (mag): 0.1105

Z (log Z/Zsun): -0.19450000000014378

z (fixed): 1.3715003312283947

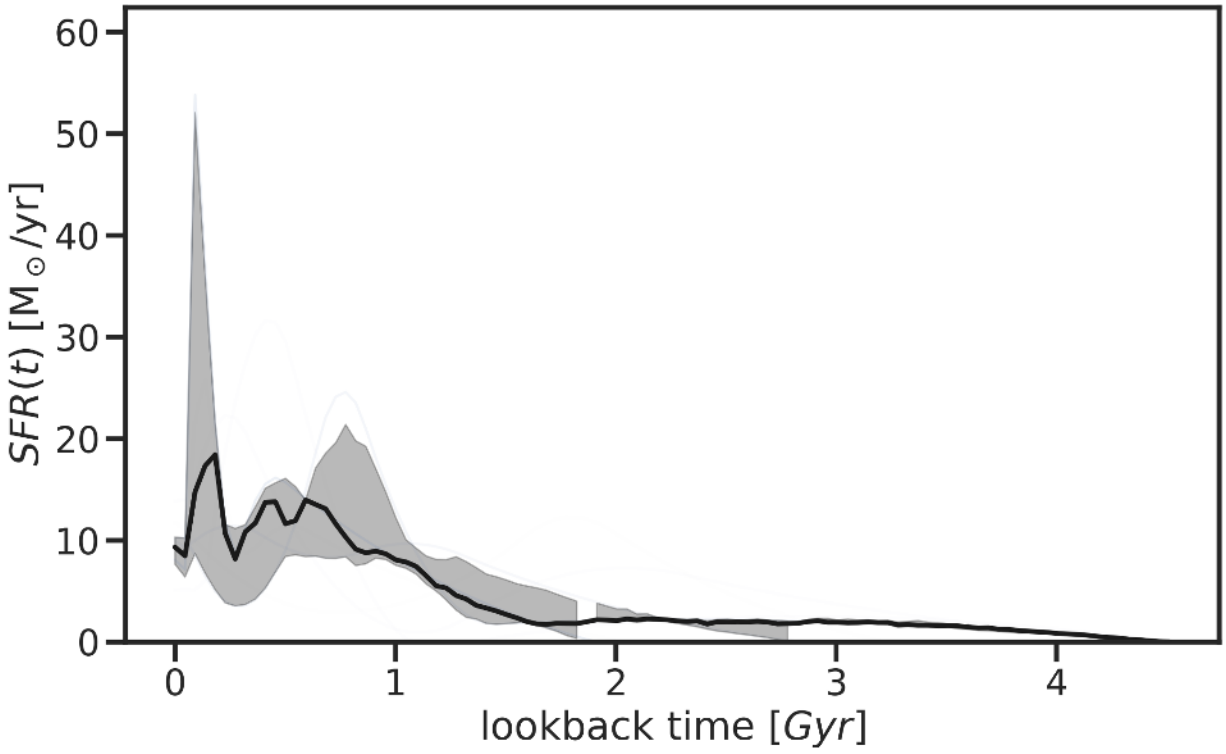

Fig.13: SFR vs lookback time distribution

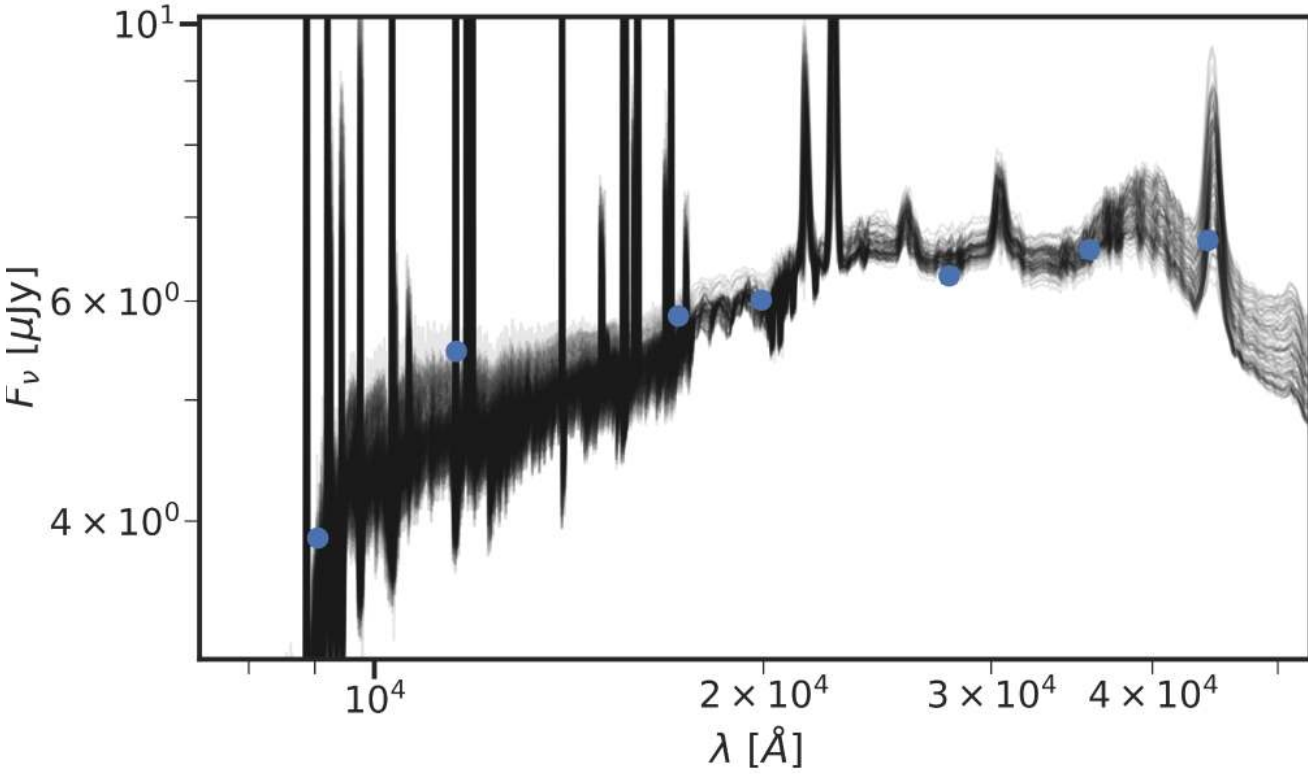

Fig.13: Flux fitting data visualization in our model spectrum

5.2 Discussion

The Sparkler Galaxy, as derived from the SED fitting using Dense Basis, is a moderately massive galaxy with a stellar mass of log10(M*/Msun) = 10.08 ± 0.04. It exhibits a moderate ongoing star formation rate (log10(SFR) = 0.9955 ± 0.01), suggesting active stellar formation, but not at an extremely high pace. The dust extinction (A_V) is low at 0.0985 mag, indicating minimal obscuration of light by dust, which allows for clearer observation of star-forming regions. The metallicity (log Z/Zsun = -0.2625 ± 0.005) is sub-solar, reflecting a relatively young stellar population with lower heavy-element enrichment, characteristic of galaxies at earlier stages of evolution. With a fixed redshift of 1.38, the galaxy is observed at a time when the universe was approximately 4.3 billion years younger.. The corner plot indicates

well-constrained posterior distributions for key parameters, and the SED fit closely matches the observed flux data across multiple wavelengths. The star formation history plot reveals a significant past burst of star formation, with a subsequent decline, aligning with expectations for galaxies transitioning from rapid to slower star formation. These findings collectively suggest that the Sparkler Galaxy is an actively forming, relatively young galaxy, but one that is starting to evolve toward a quieter phase of star formation.

References

Mowla, L. A., Iyer, K. G., Desprez, G., *et al.* 2022, "The Sparkler: Evolved High-Redshift Globular Clusters Captured by JWST," *ApJL*, **937**, L35, doi:10.3847/2041-8213/ac90ca.

Claeyssens, A., Adamo, A., Richard, J., Mahler, G., Messa, M., & Dessauges-Zavadsky, M. 2022, "Star formation at the smallest scales; A JWST study of the clump populations in SMACS0723," *arXiv e-prints*, arXiv:2208.10450, doi:10.48550/arXiv.2208.10450

Iyer, K. G., Pacifici, C., Calistro-Rivera, G., & Lovell, C. C. 2025, "The Spectral Energy Distributions of Galaxies," *arXiv e-prints*, arXiv:2502.17680, doi:10.48550/arXiv.2502.17680.

Iyer, K. G., & Gawiser, E. 2017, "Reconstruction of Galaxy Star Formation Histories through SED Fitting: The Dense Basis Approach," *arXiv e-prints*, arXiv:1702.04371, doi:10.48550/arXiv.1702.04371.

Iyer, K. G., & Gawiser, E. 2019, "Nonparametric Star Formation History Reconstruction with Gaussian Processes. I. Counting Major Episodes of Star Formation" *arXiv e-prints*, arXiv:1901.02877, doi:10.48550/arXiv.1901.02877

Approval

The internship report titled “Spectral Energy Distribution(SED) Fitting of the Sparkler Galaxy” submitted by Most. Atia Sanjida, a participant of the ICTP PWF: Physics for Bangladesh Online Summer Internship, has been found satisfactory in partial fulfillment of the requirements of the internship program. The internship was conducted under the supervision of **Lamiya Mowla** during the period **15 July 2025** to **15 October 2025**.

Supervisor

Lamiya Mowla

Wellesley College, MA, USA.